JOURNAL OF CATALYSIS 116, 422–439 (1989)

Activation of Unsupported Co–Mo Catalysts in Thiophene Hydrodesulfurization

TAMÁS I. KORÁNYI,* ISTVÁN MANNINGER,* ZOLTÁN PAÁL,* OLAF MARKS,† AND JOHN R. GÜNTER†

*Institute of Isotopes of the Hungarian Academy of Sciences, P.O. Box 77, Budapest, H-1525 Hungary; and †Institute for Inorganic Chemistry, University of Zürich, Winterthurerstrasse 190, CH-8057 Zürich, Switzerland

Received October 8, 1987; revised October 20, 1988

A series of unsupported oxidic Co–Mo catalysts with different mole fractions r = Co/(Co + Mo) was prepared by coprecipitation of solutions of $(NH_4)_6Mo_7O_{24}$ and $Co(NO_3)_2$. The calcined catalysts contain a-$CoMoO_4$ ($r = 0.5$) mixed with MoO_3 ($r < 0.5$) or with Co_3O_4 ($r > 0.5$) according to X-ray diffraction (XRD) and electron diffraction. The a-$CoMoO_4$ transforms partially into b-$CoMoO_4$ upon grinding. The higher the cobalt (r) and b-$CoMoO_4$ contents, the higher are the surface area increase and the degree of reduction of calcined catalysts during hydrogen treatment at 673 K. Electron microscopy (EM) data agree well with the surface area increase observed after reduction. X-ray photoelectron spectroscopy (XPS) shows the reduction of molybdenum rather than that of cobalt. Reduced crystalline phases cannot be identified by these techniques. Sulfidation with a mixture of H_2/thiophene following reduction caused a drastic drop in surface area but the particle size seen by EM does not increase. Weak oxythiomolybdate XRD bands appeared after slight sulfidation, most XRD signals disappeared after massive sulfidation of samples with $r = 0.5$. Cobalt promotes sulfidation of molybdenum in the bulk, but the maximum sulfidation degree was about half of the stoichiometric value. XPS shows surface cobalt enrichment, XRD and EM traces of Co_9S_8 in samples with $r = 0.38$ and 0.50. A pronounced maximum was observed in initial hydrodesulfurization (HDS) activity and hydrogenation (HYD) selectivity at medium Co content. On used catalysts, this synergism disappeared. We attribute the highest HDS activity of short-living cobalt–oxythiomolybdate(s) formed initially during sulfidation. HYD was promoted by sulfided molybdenum and by less surface cobalt.

INTRODUCTION

Co–Mo catalysts catalyze hydrodesulfurization (HDS) reaction in their sulfided state. Relatively few studies deal with the phenomena taking place when an oxidic Co–Mo sample undergoes oxide → sulfide transformation. Sulfidation can be carried out by presulfidation before runs or by the reaction mixture itself (*1, 2*). Grange (*3*) mentions that a higher HDS activity is observed during initial periods of sulfidation of oxide catalysts than over samples prepared from bulk sulfides but this higher activity is only transient.

The catalytic properties of supported and unsupported catalysts have been found to be roughly similar, thus the surface active sites were claimed to be the same (*4*). This is why we can regard unsupported Co–Mo catalysts as models of practical catalysts worth studying, especially with respect to recent developments of, e.g., carbon-supported catalysts (*5*), where the interaction between active phase and support may be quite different from that reported with Al_2O_3 supports. The true nature of the active sites on both supported and unsupported Co–Mo catalysts is still disputed (*6*). MoO_3, Co_3O_4, and $CoMoO_4$ were found by X-ray diffraction (XRD) and infrared (IR) methods in unsupported oxidic catalysts with various Co/Mo ratios (*7, 8*). $CoMoO_4$ exists in two modifications. The surface of the violet a-$CoMoO_4$ transforms to the green b-$CoMoO_4$ upon grinding. Mo-

0021-9517/89 $3.00

lybdenum occupies tetrahedral sites in the a- and octahedral sites in the b-modification (*9*).

Co_3O_4 was reduced to Co metal within minutes: approx 70% of b-$CoMoO_4$ after 2 h, while the reduction of MoO_3 just started in the bulk after 2 h H_2 treatment at 673 K (*10*). Gajardo *et al.* (*10*) calculated two types of reduction degree: one with the assumption that Mo is reduced to MoO_2, another that it is reduced to Mo metal. It is not quite clear which assumption was used for model compounds. Cimino and de Angelis (*11*) called "nearly metallic" Mo what they saw by X-ray photoelectron spectroscopy (XPS) after reduction of MoO_3 and cobalt molybdates by H_2 at 673 K for 2 h. $CoMoO_4$ also gave some metallic Co; the b-$CoMoO_4$ was reduced more easily than the a-modification (*11*). The reduction and sulfidation of MoO_3 were intensively studied by Sotani. MoO_3 + MoO_2 mixture or MoO_2 only was detected by XRD after 10 min of reaction with pure H_2 or H_2/thiophene (H_2/T) reaction mixture at 673 K, respectively (*12*). The sulfur uptake in the latter case was only 3 mass% (as measured by $BaSO_4$ gravimetry), but MoS_2 was not detected by XRD (*12*). Sotani observed MoS_2 by electron microscopy (EM) (*12*) and XPS (*13*). Only the surface of MoO_3 was sulfided, not the bulk (*13, 14*). There are two views about the sulfidation of $CoMoO_4$. Some authors claim (*15, 16*) that the products of the sulfidation are Co_9S_8 and MoS_2. However, de Beer *et al.* (*17*) identified six compounds by XRD in the product mixture; in particular, more $CoMo_2S_4$ was found than MoS_2. Co_3O_4 or metallic Co could be sulfided in the presence of molybdenum only during "normal" HDS conditions, i.e., at temperatures below 700 K (*3, 18*). The temperature-programmed reduction and temperature-programmed sulfidation of MoO_3, Co_3O_4, and $CoMoO_4$ were studied by Arnoldy and associates (*19–23*). The reducibility in H_2/Ar mixture decreased in the order Co_3O_4–$CoMoO_4$–MoO_3 (*19, 20*). The reduction of MoO_3 to MoO_2 was more rapid using H_2/H_2S as a reducing agent than in H_2/Ar; in the former case, it proceeds via an oxysulfide intermediate. The formation of MoS_2 at 650 K was slow and was restricted to surface layers only (*22*). The reduction of MoO_3 and the simultaneous reduction and sulfidation of $CoMoO_4$ and Co_3O_4 took place via O–S exchange. The role of hydrogen here is the reduction of sulfur atoms formed (*21, 22*). The rate of sulfidation of $CoMoO_4$ was very low (*21*) and the sulfidation is not complete at 675 K (heating rate: 10 K min^{-1}).

Okamoto *et al.* (*24*) found surface Mo enrichment by XPS upon sulfidation of an oxidic-unsupported Co–Mo catalyst by H_2/thiophene (H_2/T) at 673 K. On the other hand, surface Co enrichment was detected if sulfidation was carried out with H_2/H_2S. Sulfidation was only partial and MoO_2 was the only phase identified by XRD. The reduction and sulfidation of pure Co–Mo oxides have been reviewed by Grange (*3*).

Strong Mo–Al_2O_3 and weak Co–Mo interactions were suggested in alumina-supported Co–Mo catalysts. This would correspond to a "monolayer" or "bilayer" model, respectively (*2, 3, 25, 26*), which assume no crystalline Co- or Mo-oxide and/or sulfide phases on the support surface. More recent suggestions assume microcrystalline MoS_2 particles on alumina attached to it either by their basal or by their edge planes (*6*). This latter hypothesis was also confirmed by EM (*27*). However powerful high-resolution electron microscopy is as a tool (*28*), it is still not able to convincingly identify atomic groups which could be regarded as active sites responsible for catalytic activity. Therefore, we still need additional surface chemical and/or catalytic measurements to reveal their likely nature. Vacancies associated with the Co on edge sites of MoS_2 ("Co–Mo–S" structure) were proposed as active sites for HDS (*6*). The bonding of these phases to the support

via oxygen bonds was not ruled out either (*6*). Arguments based on Raman (*29*) and Auger electron (*30*) spectroscopy that oxysulfide structures exist in Mo/Al_2O_3 and $NiMo/Al_2O_3$ catalysts were published.

Massoth and Murali Dhar (*31*) proposed edge positions of MoS_2 for hydrogenation (HYD) sites, basal plane positions for cracking sites, and both positions for HDS sites. Two kinds of active sites were suggested by Yang and Satterfield (*32*). One of them is a sulfur vacancy associated with molybdenum atoms, which can facilitate HYD activity and direct extrusion of sulfur. Another site is a Brønsted acid site on which dissociated H_2S forms. Recently a linear correlation was found between the amount of coordinatively threefold unsaturated molybdenum ions in the edge plane of the MoS_2 slabs and the HYD activity (*33*). Thiophene HDS was found to be structure insensitive over sulfided molybdenum single crystals because their surface was covered with adsorbed carbon (*34*).

The HDS activity of unsupported a-$CoMoO_4$ dropped abruptly (*17*) after prereduction, similar to Al_2O_3-supported catalysts (*35*). The lower steady-state HDS activity of initially unsupported $CoMoO_4$ compared to that of supported catalysts was attributed to its low MoS_2 content after sulfidation (*17*).

The aim of the present work was to study the transient period of oxidic Co–Mo catalysts during their sulfidation with H_2/thiophene mixture. The catalytic activity was monitored by frequent sampling during this procedure. In addition, surface physicochemical measurements were also carried out on the samples in various stages of sulfidation (surface area determination, XRD, and XPS). Sulfur contents were determined by gravimetry and these results were compared with XPS data. A few electron micrographs have also been included to illustrate morphological changes. Lattice resolution images were reported elsewhere (*36*); another paper (*37*) deals with catalytic properties observed at various stages of sulfidation.

EXPERIMENTAL

Catalyst preparation. Unsupported catalysts were prepared in mole fractions of r = Co/(Co + Mo) = 0, 0.17, 0.38, 0.50, 0.68, and 1. Stoichiometric quantities of $(NH_4)_6Mo_7O_{24} \times 4H_2O$ (AHM) and $Co(NO_3)_2 \times 6H_2O$ (Reanal puriss grade each) were dissolved in water. NH_3 (10%) excess was added to the AHM solutions in order to promote MoO_4^{2-} formation by shifting of the polymolybdate $\rightleftharpoons$ monomolybdate equilibrium. The mixed solutions were dried at 390 K and calcined in air at 723 K for 4 h. MoO_3, a-$CoMoO_4$, and Co_3O_4 model compounds for XPS measurements were the products of our catalyst preparation procedure (r = 0, 0.50, and 1, respectively). Co_9S_8 was prepared from the stoichiometric mixture of its elements by heating at 920 K for 3 days *in vacuo*. MoS_2 and $CoSO_4$ were commercial products (Reanal puriss each).

Catalyst activation. Oxidic (100 mg) (calcined) catalysts were placed into a 4 mm i.d. Pyrex glass tube reactor between quartz wool. This reactor was operated as a continuous-flow apparatus (*37*). A special reactor (Fig. 1) was used before IR and XPS measurements, which permitted the flooding of the activated catalyst sample (*38*) with paraffin oil (for IR) or *n*-octane (for XPS) in order to avoid the contamination of the samples with air, which could alter the surface structure and sulfur content (*39*). The contact of sulfided samples with air cannot cause much experimental error, since a sample reduced for 2 h in the reactor gave the same high surface area after transferring to the BET system in air as *in situ* reduction in the BET system in some cases. Prereduction of the catalysts was carried out at 673 K with 40 ml/min H_2 stream velocities for 2 h preceding the reaction. The HDS reaction (which also provided sulfidation) was performed with a

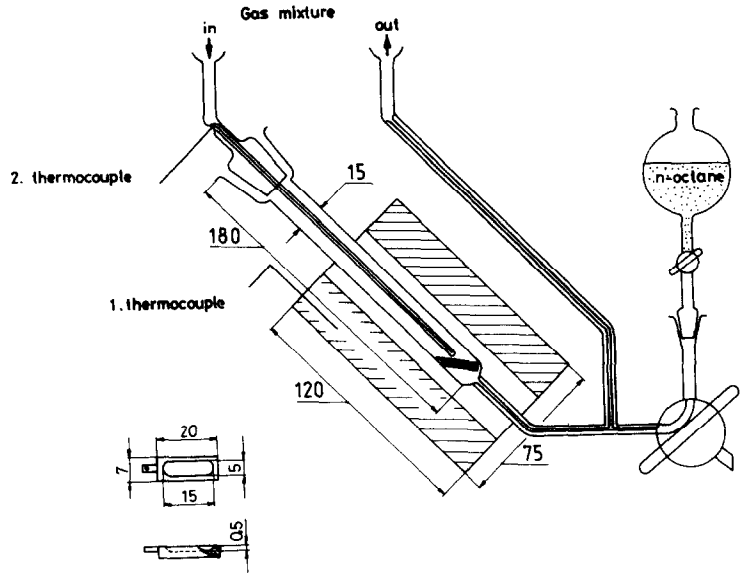

FIG. 1. Special reactor for flooding of the XPS and IR samples after various treatments with the XPS sample holder (lower left). Dimensions are given in millimeters.

35/1 H_2/T mixture also at 673 K with 40 ml/min velocity. The time-on-stream was 70 min (70 min H_2/T). Used catalysts were cooled to room temperature in a N_2 stream. Catalytic properties (thiophene conversion (X (%)) and hydrogenation selectivity (HYD = (isobutane + n-butane)/(ΣC_4 hydrocarbon) ratios of the product mixture) were measured gas chromatographically, in detail, see in Ref. (*37*).

X-ray diffraction. The measurements were carried out in a DRON 2 diffractometer in the 5°–80° range with Co$K\alpha$ and Co$K\beta$ radiations. The resolution was 0.05°. The identification of the crystal phases was carried out with the literature data of the Powder Diffraction File of JCPDS. The samples were stored in air for an extended period before measurements.

Specific surface area and degree of reduction. The specific surface areas of the catalysts were measured gravimetrically with the BET method (N_2 adsorption) an a Sartorius 4012 microbalance. The H_2 reduction was carried out *in situ* in the BET apparatus (T = 673 K, H_2 flow); thus, the degree of reduction could be determined from the mass loss. The sulfided samples contacted with air during their transport from the flow reactor to the BET system (for maximum 30 min).

The *sulfur content* of the sulfided catalysts was determined by a gravimetric method used for the measurement of sulfur content of pyrites. The ice-cooled 50- to 100-mg sample was left in 10 ml inverse aqua regia ($HCl:HNO_3$ = 1:3) overnight. The solution was evaporated three times to dryness in 10 ml 20 mass% HCl each, then diluted to 60 ml. The warm solution was mixed with a warm aqueous solution of $BaCl_2$ (Reanal puriss grade), whereupon $BaSO_4$ was precipitated. The wet solution stayed overnight, then it was filtered through an ashless filter paper. The precipitate with the filter paper was burned, glowed, and weighed.

Electron microscopy and electron diffraction (ED). A transmission electron microscope JEOL JEM 200-CX with top entry goniometer stage and ultrahigh resolution objective pole piece was used. It was operated at 200 kV. Samples were prepared by suspension in bidistilled water, dispersed

by an ultrasonic treatment, and then dried on holey-carbon support films.

X-ray photoelectron spectroscopy. Calcined samples (60–80 mg) were pressed by ~500 bar into the 15 × 5 × 0.5-mm useful volume of a stainless-steel XPS sample holder (Fig. 1, lower left). Samples with sample holder were placed into the reactor shown in Fig. 1 in the case of activation (reduction and/or sulfidation). The flooding of the activated sample after cooling below 373 K in a N_2 stream was carried out in the same reactor by freshly distilled *n*-octane (Reanal puriss), which was dried over P_2O_5 previously. The samples were stored under *n*-octane till the XPS measurements (maximum for 3 days). A KRATOS ES 300 XPS equipment was used. The exciting radiation was Al$K\alpha$ (15 kV 10 mA). The samples were picked out of *n*-octane and were placed within seconds into the XPS apparatus. Calcined samples or model compounds were introduced into the XPS apparatus without flooding. The samples were evacuated to $\sim 10^{-6}$ Pa before measurement in three steps within 30 min. The spectra of the C 1*s*, O 1*s*, Mo 3*d* + S 2*s*, S 2*p*, and Co 2*p* levels were recorded. The number of scans was 5, 3, 10, 10, and 20, respectively; the sequence of recording of spectra was the same for all catalysts in order to reduce the error associated with carbon contamination and charging of the sample (*18, 40*). The C 1*s* = 284.4 eV internal reference line was used to calibrate the spectra (*16*). The accuracy in the determination of the binding energy (BE) of single peaks was ±0.4 eV.

Quantitative analysis of XPS spectra. The intensity of an XPS signal of an element *x* is described by the relationship (*41*)

$$I_x = n_x \cdot \sigma_x \cdot T(E_x) \cdot \lambda(E_x) = n_x \cdot K_x, \quad (1)$$

where n_x is the concentration of the element, σ_x is the photoelectron cross section (*42*) corrected with the asymmetry parameter β (*43*), $T(E_x)$ is the transmission factor depending on the kinetic energy E_x, and $\lambda(E_x)$ is the mean free path (escape depth) of the corresponding photoelectron. The values in our equipment are $\lambda \sim E_x^{0.75}$ (*44*) and $T \sim E_x$, therefore,

$$K_x \sim \sigma_x \cdot E_x^{1.75}. \quad (2)$$

The angle between X-rays and photoelectrons is ~90°, thus the corrected photoelectron cross section is

$$\sigma_{corr} = \sigma_{nl}\left(1 + \frac{\beta_{nl}}{4}\right). \quad (3)$$

From Eqs. (1–3),

$$n_x = \frac{I_x}{K_x} \sim \frac{I_x}{\sigma_{corr} \cdot E_x^{1.75}}. \quad (4)$$

Absolute surface concentrations cannot be calculated from Eq.(4), but their ratios can. Atomic ratios $n_{Co}/(n_{Co} + n_{Mo})$ and $n_S/(n_{Co} + n_{Mo})$ seen by XPS were calculated and referred to as "surface" ratios. These data originate to the escape depth of the photoelectrons and thus represent the concentration ratios in the outer layers of the catalyst surface. The signal intensity I_{Co} is the sum of the intensities of the Co $2p_{3/2}$ and satellite lines, I_S is the sum of intensities of all (S^{2-} and S^{6+}) S 2*p* levels of the sample, and I_{Mo} is the sum of intensities of Mo $3d_{3/2}$ and Mo $3d_{5/2}$ peaks. The $3d_{5/2}$ peak overlaps with the S 2*s* peak in the spectra of sulfided samples; therefore, the intensity of the S 2*s* band must be deducted from the intensity of the Mo 3*d* + S 2*s* complex band. The $I_{S\,2p}/I_{S\,2s}$ ratio calculated from the values of σ_{corr} is 1.507 and the ratio measured in the spectrum of Co_9S_8 is 1.462. Therefore two-thirds of I_S was subtracted from the intensity of the complex band to get I_{Mo}.

RESULTS

XRD. The results of the XRD measurements are shown in Table 1. The phases observed in calcined samples are in accordance with the IR results (*5*). The presence of a-$CoMoO_4$ is confirmed by the violet color of all calcined, cobalt containing catalysts. Some samples were ground after calcination to induce the a-$CoMoO_4$ → b-

TABLE 1

Crystalline Phases Identified by XRD after Various Treatments

Treatment	$r = 0$	a-0.17	a-0.38	a-0.50	b-0.50
Calcined	MoO_3	MoO_3 + a-$CoMoO_4$	MoO_3 + a-$CoMoO_4$	a-$CoMoO_4$	a-$CoMoO_4$
2 h H_2	MoO_3	MoO_3	MoO_3 + a-$CoMoO_4$	a-$CoMoO_4$	a-$CoMoO_4$
1 min H_2/T	MoO_3	MoO_3	MoO_3 + a-$CoMoO_4$	a-$CoMoO_4$ + $CoMoS_{0.17}O_{3.83}$ trace	a-$CoMoO_4$ + $CoMoS_{0.17}O_{3.83}$ trace
10 min H_2/T	MoO_3	MoO_3	a-$CoMoO_4$ + $CoMoS_{1.02}O_{2.78}$ trace	a-$CoMoO_4$ trace	a-$CoMoO_4$ trace
70 min H_2/T	MoO_3	MoO_3	a-$CoMoO_4$ trace	Two peaks[a]	Two peaks[a]

Note. Source: JCPDS Powder Diffraction File, International Center for Diffraction Data, Swarthmore, PA. The individual diffractions were taken from the following file cards: MoO_3 (orthorhombic) 5–508; $CoMoO_4$ (monoclinic) 21–868; Co_9S_8 (cubic) 19–364; $CoMoS_{1.02}O_{2.78}$ 16–27; $CoMoS_{0.17}O_{3.83}$ 16–61; MoO_2 (monoclinic) 5–452.

[a] Two low intensity peaks only. One of these peaks is the most intensive peak of Co_9S_8.

$CoMoO_4$ phase transition. The color changed to dark green, but the XRD bands of a-$CoMoO_4$ did not change to the bands of b-$CoMoO_4$ (Table 1). Trifiro *et al.* (*9*) attributed their similar results to the fact that the a → b transition occurred on the surface only. Note that MoO_3 and $CoMoO_4$ were also present after reduction; the XRD line broadening pointed to their poor crystallinity. However, data were insufficient to calculate crystallite sizes. Neither MoS_2 nor Co_9S_8 could be identified with sufficient certainty after intensive sulfidation. Considering also the IR (*8*) and EM (*36*) results, we believe that Co_9S_8 is present in the "two peaks" phase, but one single peak cannot be taken as a firm evidence. More than one reflection shows the presence of cobalt–oxythiomolybdates in the early stage of sulfidation of samples with high $CoMoO_4$ content. The sum of oxide and sulfide ions is 4 or 3.8 in the two phases identified according to the Powder File (File Numbers 16–27, 16–61, see also Table 1). It seems that a-$CoMoO_4$ is reduced and sulfided more easily, than MoO_3 under the same conditions. The poor crystallinity of the products of the sulfidation of $CoMoO_4$ must be emphasized.

Electron microscopy and electron diffraction. Figure 2. shows a set of micrographs of a catalyst with r = a-0.50 after various treatments. Figure 2a exhibits a rather transparent, flat, platelet-like a-$CoMoO_4$ particle (size 1–3 μm). Figure 2b shows particles of a-0.50 catalyst after 2 h H_2 reduction. The sample is nonuniform in particle sizes, but the original particle has broken down into an aggregate of distinctly smaller individual grains. Primary particle sizes are approx 0.02 μm (Fig. 2b). The electron diffraction pattern of the reduced sample is characteristic of a polycrystalline one; some rather distinct spots indicate the presence of crystalline $CoMoO_4$. Some unidentified additional reflections were also found, which can, perhaps, be attributed to reduced species. Figure 2c shows the particles of prereduced $r = 0.50$ catalyst after 10 min H_2/T. The primary crystallite sizes do not increase compared to those of the reduced catalyst. Broader, diffuse electron diffraction rings appear with the reduced sample, but the strongest ring corresponds again to the strongest reflection of $CoMoO_4$. Even after a low degree of sulfidation, MoS_2 appears in the electron micrographs. In the samples after 70 min H_2/T electron microscopy and diffraction prove the presence of Co_9S_8 in addition to MoS_2

FIG. 2. Electron micrographs of a-0.50 catalyst after various treatments; (a) calcined; (b) reduced (2 h H_2); (c) sulfided by 10 min H_2/T after reduction; (d) sulfided by 70 min H_2/T after reduction. The fibrous material seen on (d) is elementary sulfur.

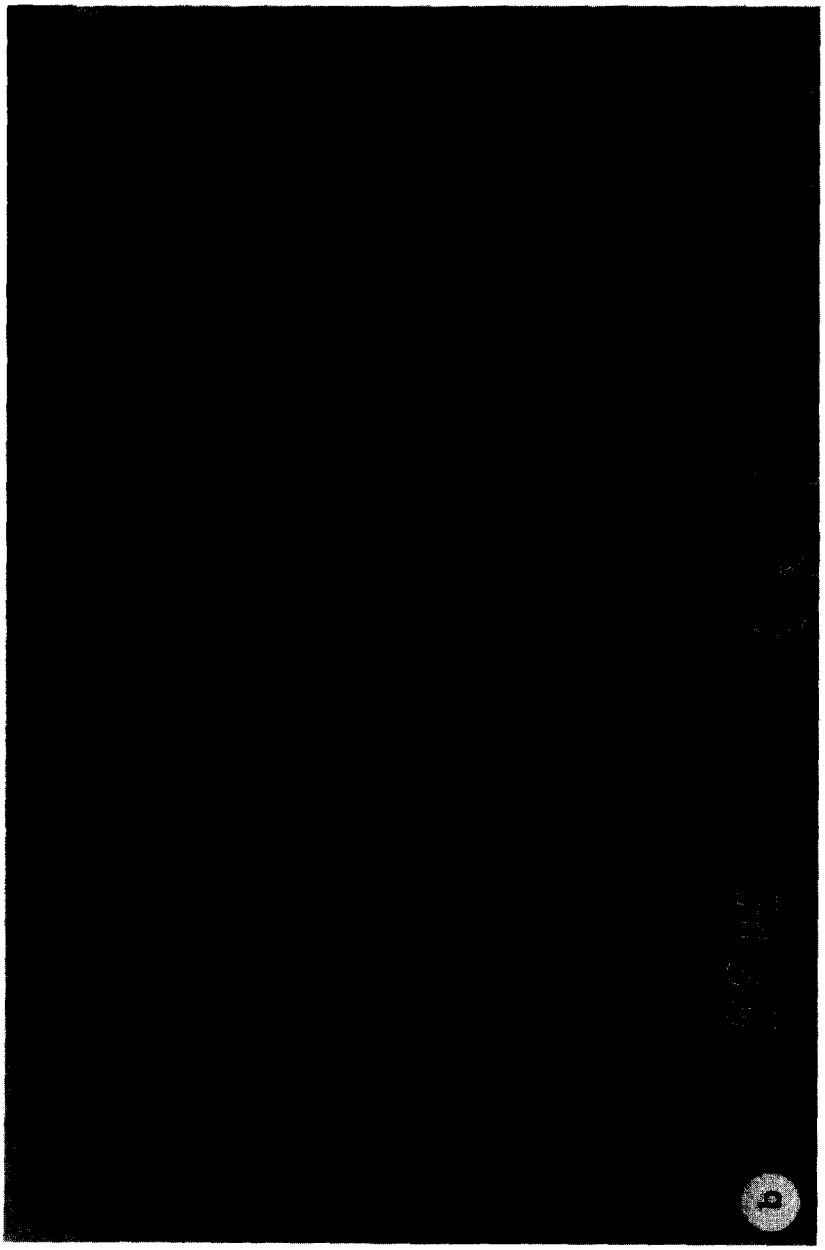

FIG. 2—*Continued.*

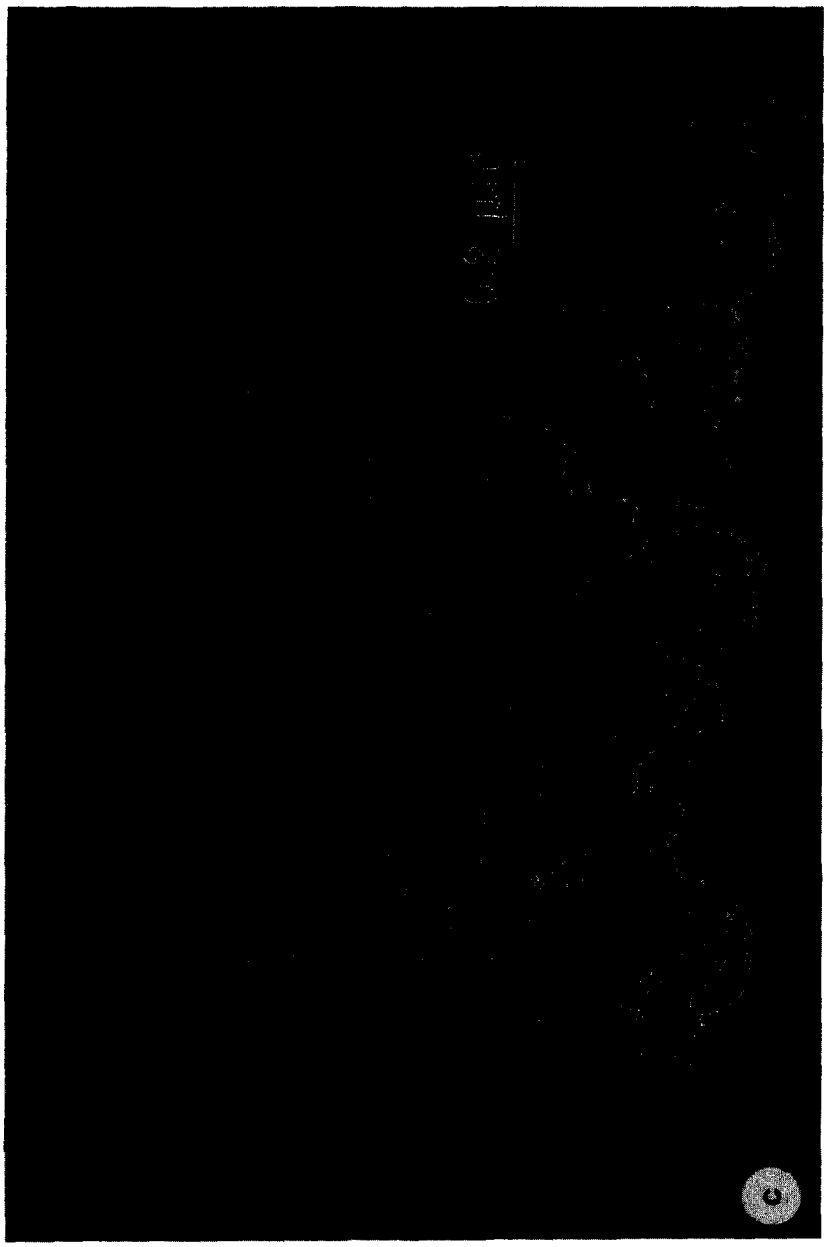

FIG. 2—*Continued.*

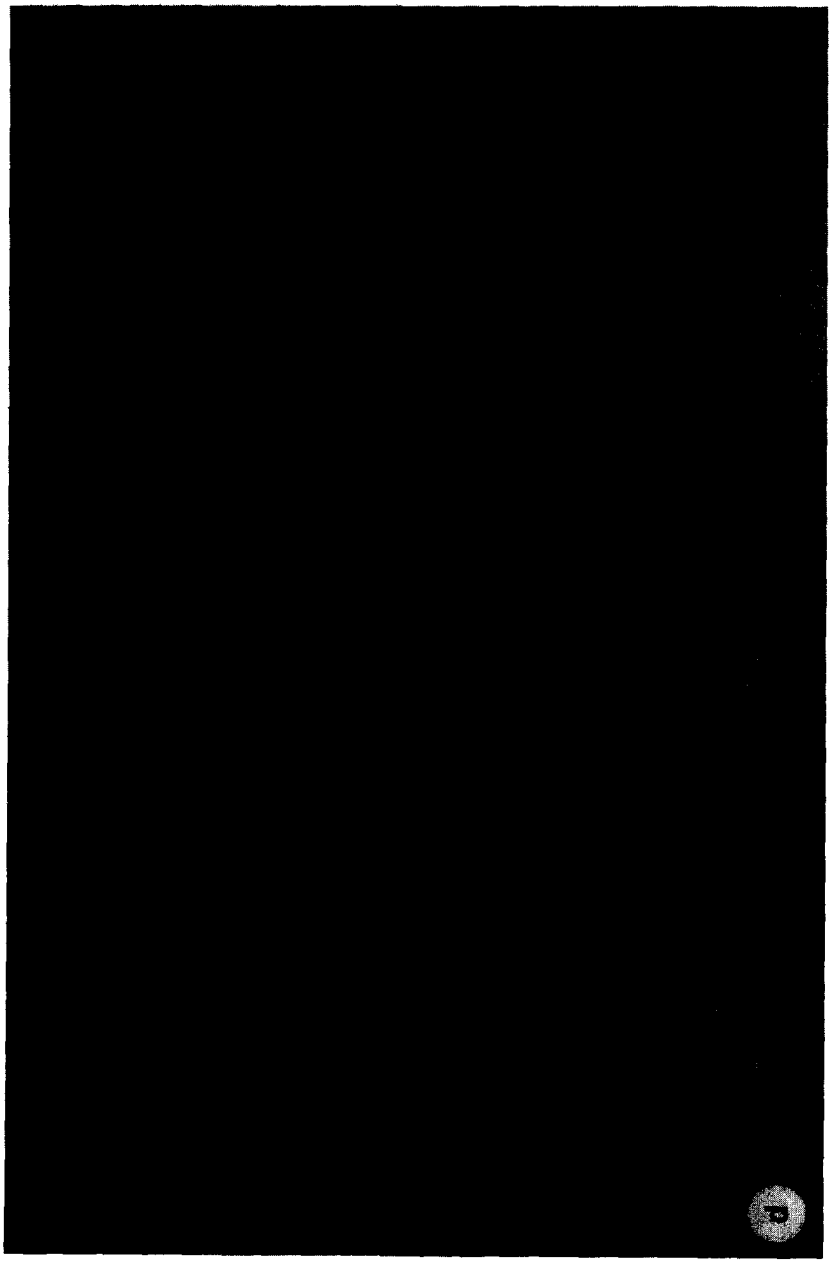

FIG. 2—*Continued.*

(*36*). The channels disappear almost entirely. In addition to the catalyst grains, a fibrous material unstable in the electron beam appears which can be identified by its ED pattern as elementary S (Fig. 2d).

Specific surface areas and the degree of reduction. The results of specific surface area measurements are shown in Fig. 3. Samples containing b-$CoMoO_4$ have slightly larger surfaces than those containing a-$CoMoO_4$ in the calcined state. A very pronounced surface increase is observed after reduction. A larger increase occurs with higher r values or with catalysts containing b-$CoMoO_4$. The specific surface areas of samples of various compositions become nearly identical after sulfidation (Fig. 3). The extent of reduction was estimated using both assumptions of Gajardo *et al.* (*10*), as shown in lines 3 and 4 of Table 2. Catalysts with higher r values or those containing b-$CoMoO_4$ are reduced to a higher extent. The reduction is not stoichiometrically complete even assuming that it stops at Mo(IV), except for $r = 0.68$. Thus, our experiments show that at least in this case, a species with lower than four-valence Mo must have been formed, like that found by Valyon and Hall (*45*) with supported Mo catalyst.

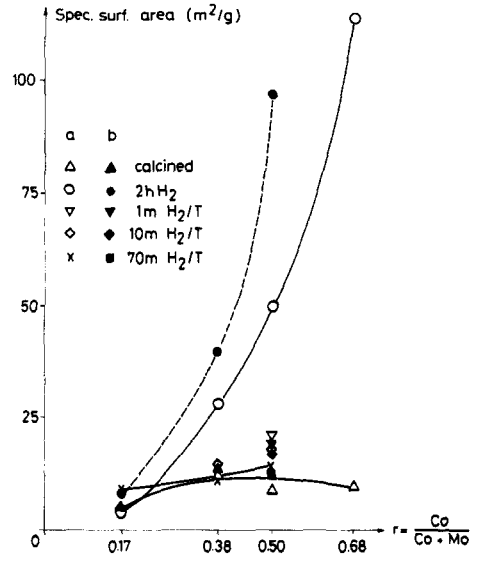

FIG. 3. Specific surface areas (m^2/g) of calcined, reduced, and sulfided catalysts. Symbol in means minutes.

Sulfur content. The sulfur contents as determined by gravimetric measurements (Fig. 4) showed a lower degree of sulfidation than the theoretically attainable bulk values (37–40 mass% S). A time-on-stream of 20–25 min ought to be sufficient for stoichiometrically complete sulfidation provided that all sulfur atoms split off the feed remained on the catalyst. However, only a fraction of them was used for catalyst sulfidation (Fig. 4), in agreement with the results of other papers (*37, 46*). Sulfur uptake is very rapid at the beginning of sulfidation (Fig. 4, values at 1 min H_2/T) in accordance with reports on supported catalysts (*26, 35*). The higher the MoO_3 content of the samples (in addition to $CoMoO_4$), the lower is the sulfur uptake. After a massive sulfidation, elementary sulfur is also present (cf. Fig. 2d).

XPS spectra. The XPS spectra of six model compounds with calibrated BE are shown in Fig. 5. The Co $2p_{3/2}$ band of a-$CoMoO_4$ appears at BE = 781.4 eV, which was the value assigned to Co^{2+} ions in the oxide environment. This band has a weak shake-up satellite structure at BE higher by approximately 6 eV than the main peak in Co_3O_4. This satellite is strong in $CoMoO_4$ and $CoSO_4$ (*3, 39, 47*). The peak at BE = 777.9 eV belongs to the Co $2p_{3/2}$ band of Co_9S_8 and to Co^{2+} ions in the sulfide environment or to metallic Co (*3, 16, 48*). Co_9S_8 model compounds may have reoxidized after having contacted with air subsequent to preparation. This could be seen on its color and on the appearance of a small shoulder in its Co $2p_{3/2}$ band. The C 1*s* BE = 284.4 eV was found to be more suitable as a reference line in our samples than the O 1*s* = 530.3 eV line (suggested by Gajardo *et al.* (*18*)). The O 1*s* doublet line of $CoMoO_4$ appears also in the spectrum of $NiMoO_4$ (*41*). The spin–orbit splitting of the Mo 3*d* band is 3.1 eV both in oxide (a-$CoMoO_4$, MoO_3)

TABLE 2

The Degree of Reductions of Unsupported Catalysts after 2 h H_2

	r						
	a-0.17	b-0.17	a-0.38	b-0.38	a-0.50	b-0.50	0.68
Mass loss (%)	0.7	2.5	2.6	4.4	4.2	9.0	19.0
Oxygen loss (mole% of the total oxygen present)	2.15	7.65	8.48	14.4	14.4	30.7	66.8
Reduced $CoMoO_4$ (a)	8.42	29.9	12.5	21.1	14.4	30.7	54.3
(mole%) (b)	16.8	59.8	25.0	42.5	28.8	61.3	108.6

Note. assumptions: (a) MoO_3 is not reduced, $CoMoO_4$ and Co_3O_4 are reduced to metal(s); (b) MoO_3 is not reduced, $CoMoO_4$ is reduced to MoO_2, and Co_3O_4 is reduced to metal. After Gajardo *et al.* (*10*).

and in sulfide (MoS_2) surrounding and is in accordance with (*11, 16, 40, 49*). The bands at 235.5 eV (Mo $3d_{3/2}$) and 232.4 eV (Mo $3d_{5/2}$) were assigned to Mo^{6+} species in an oxidic surrounding, those at 232.2 eV (Mo $3d_{3/2}$) and 229.1 eV (Mo $3d_{5/2}$) to Mo^{4+} species in a sulfidic surrounding on the basis of model compound spectra of a-$CoMoO_4$, MoO_3, and MoS_2. The chemical shift between the Mo $3d$ bands of MoO_2 and MoS_2 is only 0.4–0.7 eV (*24, 49*); therefore, it is not easy to decide whether the Mo^{4+} species are in oxidic or sulfidic environments. The band of S $2s$ partially overlap with the Mo $3d$ levels (226.5 eV). The binding energies 226.5 eV (S $2s$) and 162.0 eV (S $2p$) were assigned to S^{2-} species, on the basis of the spectrum of MoS_2. These BE values do not depend on the nature of species (Mo or Co) being chemically bonded to sulfur (*16, 48*). The BE = 168.2 eV (S $2p$) was assigned to S^{6+} from the spectrum of $CoSO_4$. The S $2s$ peak of the sulfate band can be seen in this spectrum too. Both sulfate bands appear also in the spectrum of Co_9S_8; these and also the Co $2p_{3/2}$ peak point to a partial oxidation of Co_9S_8 after preparation. The band at approx 158 eV in the S $2p$ spectrum of $CoSO_4$ is likely to belong to the sulfur contamination of the sample holder. The measured binding energies of model compounds are within the range of data given in various literature sources (*11, 15, 16, 24, 40, 47, 49*).

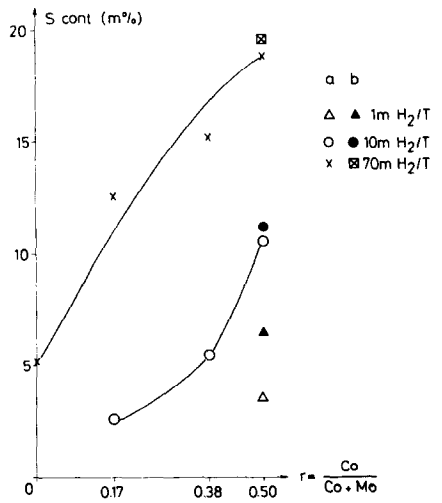

FIG. 4. Sulfur content in mass percent (S cont (m%)) of sulfided catalysts.

Figure 6 shows the XPS spectra of mixed Co–Mo-calcined catalysts (pure ones, r = 0, 0.50, 1 were shown in Fig. 5). The Co $2p$ and Mo $3d$ bands clearly indicate that these metals are in +2 and +6 oxidation state, respectively. The O $1s$ doublet line—which can be regarded as characteristic of $CoMoO_4$—appears in the spectra of all catalysts of Fig. 6.

The XPS spectra of reduced catalysts

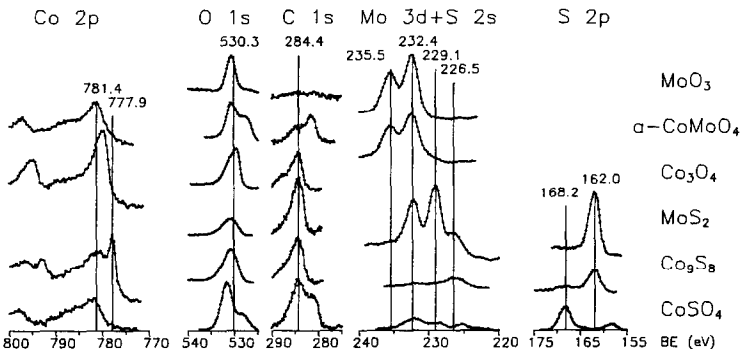

FIG. 5. XPS spectra of model compounds.

(Fig. 7) show that mainly molybdenum was reduced: a shoulder appears at 229.1 eV in the Mo 3*d* spectra which can be assigned to Mo^{4+} species. The intensity of this band compared with that of Mo^{6+} increases with increasing cobalt content in accordance with our gravimetric measurements (Table 2). Surprisingly, the reduction of cobalt does not appear in the XPS spectra: there is no shoulder at 777.9 eV. Contrary to this, the relative intensity of the satellite band at about 787 eV related to the main, 781.4 eV band is higher in reduced catalysts than in calcined ones (Fig. 7 vs Figs. 5 and 6). This phenomenon indicates a decreasing relative amount of low-spin Co^{3+}—that is Co_3O_4—compared to high-spin Co^{2+} (*40, 47*) and an increasing quantity of metallic Co (*48*). The relative intensity of the left-side peak in the O 1*s* doublet line decreases with increasing cobalt content in reduced catalysts (Fig. 7) compared to the intensity ratios of O 1*s* band in calcined samples (Figs. 5 and 6). The doublet character of O 1*s* peak disappears in the spectra of reduced catalysts $r = 0.68$ and $r = 1$. This singlet also indicates that these samples are reduced to the highest degree in accordance with the data in Table 2.

The XPS spectra of sulfided catalysts (Fig. 8) show that the sulfidation of molybdenum is more likely than that of cobalt similarly to their reduction (Fig. 7). More precisely, the Mo^{4+} $3d_{5/2}$ shoulder (229.1 eV)—which appears first after reduction (Fig. 7)—becomes well separated from the sum of Mo^{6+} $3d_{5/2}$ (232.4 eV) and Mo^{4+} $3d_{3/2}$ (232.2 eV) bands. The reduction or sulfidation of cobalt is more pronounced in sulfided catalysts than in reduced samples, but Co in the oxidic environment still predominates: the intensity of the Co^0 or Co^{2+} (sulfide) $2p_{3/2}$ (777.9 eV) shoulder is higher than in reduced samples (Fig. 7), but its intensity

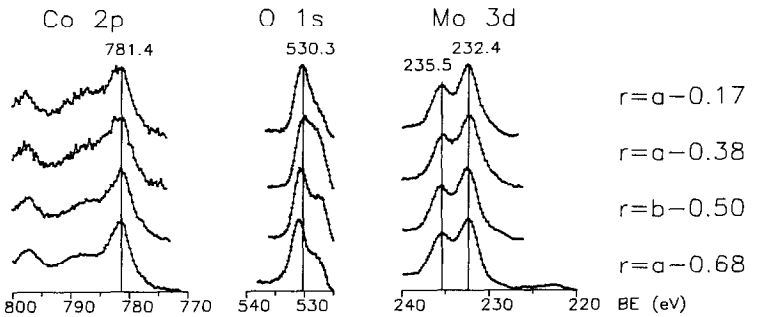

FIG. 6. XPS spectra of calcined catalysts.

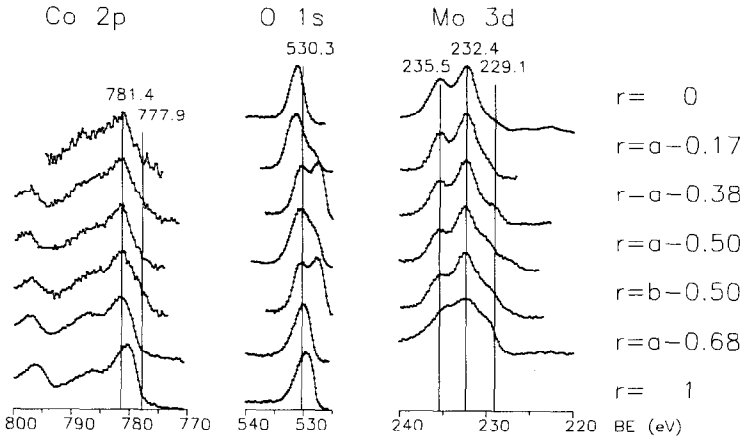

FIG. 7. XPS spectra of reduced catalysts.

never exceeds that of the Co^{2+} (oxide) $2p_{3/2}$ (781.4 eV) band. The intensity of Mo^{4+} $3d_{5/2}$ (229.1 eV) bands sometimes exceeds that of Mo^{6+} $3d_{3/2}$ (235.5 eV) bands (considering also the theoretical 5 : 3 ratio). Surprisingly, the higher the molybdenum content of our sulfided catalysts, the higher is the Mo^{4+} : Mo^{6+} intensity ratio. The surface of these catalysts (except $r = 1$) is sulfided to a high degree according to XPS results (see S 2*p* and S 2*s* signals) whereas the bulk is sulfided to a lower extent as shown by the bulk sulfur content (Fig. 4). O 1*s* peaks of sulfided catalysts are all singlets; therefore, they are not shown.

Surface composition as determined by XPS. The results of quantitative analysis are shown in Fig. 9. The calcined catalysts a-0.17 and a-0.38 show a surface cobalt enrichment related to bulk composition, contrary to (*24*). The calcined sample a-0.68 exhibits surface cobalt depletion. (The straight, diagonal line would correspond to identical surface and bulk Co/(Co + Mo) ratios.) Reduction has no considerable effect to surface cobalt ratios. Sulfidation causes a very significant increase in the surface Co/(Co + Mo) ratio of catalysts r = a-0.17, a-0.38, and a-0.50, but does not change that of r = b-0.50 and a-0.68. This

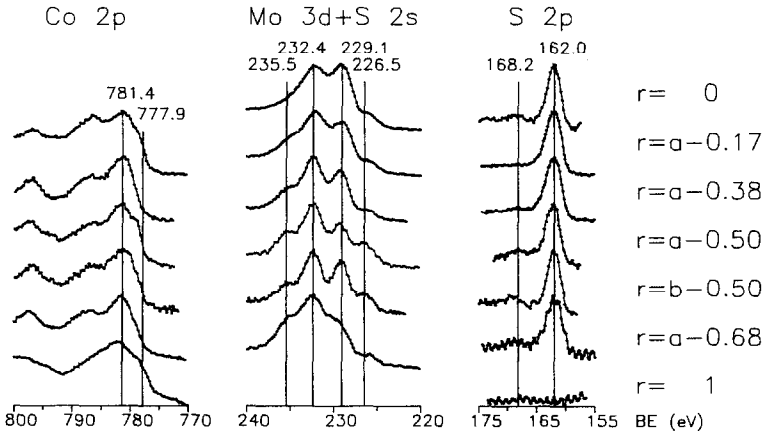

FIG. 8. XPS spectra of sulfided catalysts.

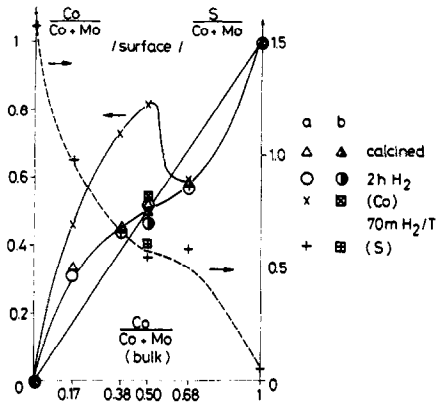

FIG. 9. Surface Co/(Co + Mo) and S/(Co + Mo) mole fractions as measured by XPS related to bulk Co/(Co + Mo) compositions.

phenomenon can be connected with the different initial degree of reduction of these catalysts before sulfidation. The latter catalysts (b-0.50, a-0.68) were reduced to a higher extent before their contact with thiophene than the former ones (a-0.17, a-0.38, a-0.50) (see Table 2). This reduction practically does not continue further during the reaction as shown by their XPS spectra (compare Co 2*p* and Mo 3*d* spectra in Figs. 7 and 8). The reduction of catalysts r = a-0.17, a-0.38, and a-0.50 proceeds during sulfidation as can be seen from the Mo 3*d* spectra of these samples before (Fig. 7) and after (Fig. 8) HDS. The surface S/(Co + Mo) ratios of sulfided catalysts show S-shaped curves similarly to the surface Co/(Co + Mo) ratios of the same samples. Catalysts with high surface Co enrichment exhibit relatively low S/(Co + Mo) ratios and catalysts where sulfidation do not cause high Co enrichment (b-0.50, a-0.68) show normal S/(Co + Mo) ratios (i.e., its value coincides with an imaginary straight line connecting the S/(Co + Mo) ratios of $r = 0$ and $r = 1$ catalysts).

Catalytic properties. One of the most interesting questions concerns how these identified bulk and surface species behave in HDS reaction of thiophene. Thiophene HDS activities (Fig. 10) of samples used subsequently for XPS measurements have maxima just after the reaction starts (2 min H_2/T). The highest activity was obtained at composition $r = 0.50$, where cobalt–oxythiomolybdates were identified by XRD at the beginning of the reaction (Table 1). The extremely high synergy at $r = 0.50$ is even more conspicuous, if the conversions are plotted as a function of surface Co/(Co + Mo) ratios as measured by XPS (dashed line in Fig. 10). The conversions exhibit a decreasing, slightly S-shaped curve at a later period of the run (70 min H_2/T). Catalysts containing both metals show nearly the same conversions (5–10%) at 70 min H_2/T.

Hydrogenation selectivities (Fig. 11) are similar to conversion plots, but two differences are striking: the maxima are not exactly at composition $r = 0.50$ and the catalyst $r = 0$ exhibits anomally high values. This exceeds the HYD selectivity of $r = 0.17$ at the start (2 min H_2/T) but is the highest of all samples at the end (70 min H_2/T) of the run.

Another interesting picture can be seen if the catalytic properties are plotted as a function of the surface S/(Co + Mo) ratios after 70 min H_2/T (i.e., *at the end of the run*). Figure 12 shows that the conversions

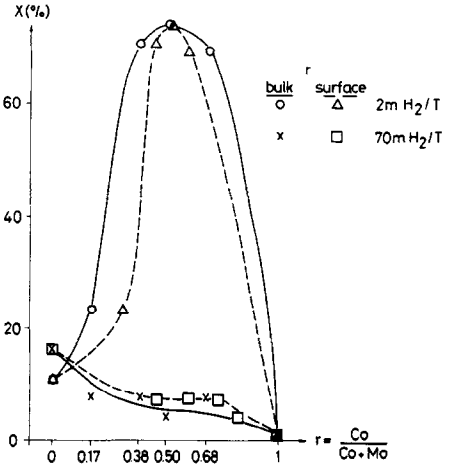

FIG. 10. Thiophene conversions (X (%)) measured over XPS samples as a function of the bulk and surface Co/(Co + Mo) ratios.

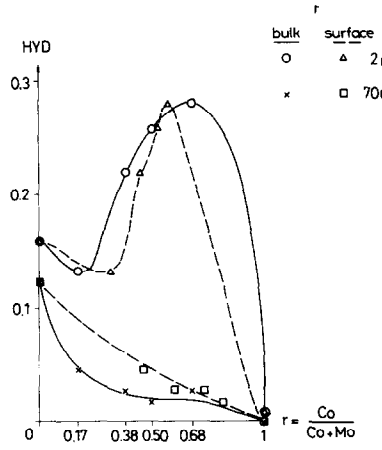

FIG. 11. Hydrogenation (HYD = (*n*-butane + *i*-butane)/ΣC_4 products) selectivities measured over XPS samples as a function of the bulk and surface Co/(Co + Mo) ratios.

represent nearly the mirror image of the corresponding plot as a function of the surface Co/(Co + Mo) ratio. The same is true for HYD selectivities (cf. Figs. 10 and 11). Note that Fig. 12 combines catalysts with various r values; $r = 0$ is at the right-hand side, $r = 1$ at the left-hand side of the figure.

DISCUSSION

The *calcined, oxidic form* of unsupported Co–Mo catalysts contains a-$CoMoO_4$ ($r = 0.50$) mixed with MoO_3 ($r < 0.50$) or with Co_3O_4 ($r > 0.50$) according to our IR spectra (*8*), XRD (Table 1), EM (Fig. 2), and ED measurements in accordance with our previous results (*8*). This is not in complete agreement with the literature, because Lipsch and Schuit (*7*) found $CoMoO_4$ only at a composition of $r = 0.50$. Above a value of $r = 0.17$, the specific surface increases already in the calcined state with increasing r (Fig. 3). This effect is concomitant with surface cobalt enrichment in the case of catalysts with $r < 0.50$ (Fig. 9), contrary to the results of Okamoto *et al.* (*24*).

Reduction has a very marked effect on the specific surface areas (Fig. 3). This is in good agreement with the EM pictures shown (Fig. 2). Reduction in H_2 seems to break up the $CoMoO_4$ particles into an agglomerate of smaller grains which give the contour of the whole original particle (pseudomorphism). This means that solid-state transformations occurring during reduction must cause formation of channels in the $CoMoO_4$ grains as the electron diffraction patterns show that the bulk has remained $CoMoO_4$. When less cobalt is present ($r = 0.17$), the reduction is slower, consequently the specific area does not increase upon H_2 treatment. It would be of interest to check "channel formation" by EM.

Mass loss during reduction (Table 2) as well as changes in the position and satellite structure of XPS lines (Figs. 5 to 7) can give information on the degree of reduction, i.e., on the likely valence states of Co and Mo ions. The XPS observations show that first of all Mo will be reduced and that this process is enhanced by the presence of Co (Fig. 7). Here the reduction of cobalt cannot be excluded either. Since no reduced phase was detected, the mass losses and XPS results support the assumption that anion vacancies are formed mainly on Mo atoms during reduction in accordance with (*2, 7, 26*). Both types of data (mass loss and XPS) show that the b-modification of

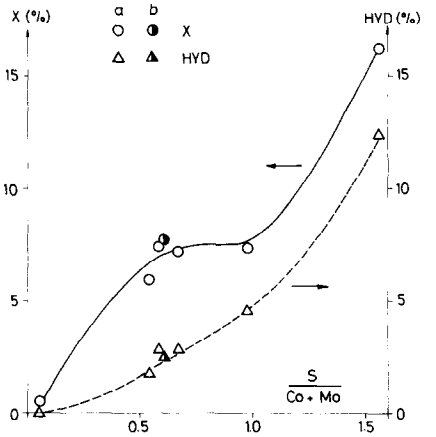

FIG. 12. Thiophene conversions (X (%)) and HYD selectivities measured over 70 min H_2/T XPS samples as a function of the surface S/(Co + Mo) ratios.

$CoMoO_4$ is reduced more readily than its a-modification in accordance with (*11*). All XPS data show that Mo^{6+} is still present in considerable amounts along with Mo^{4+} after reduction, contrary to results of (*11, 12*). Our experiments do not show oxidation states of Mo lower than four with pure Mo (*45*), but such species can be assumed in Co–Mo catalysts and are certainly present in the sample with $r = 0.68$ (Table 2).

The *sulfidation* with H_2/thiophene decreases the crystallinity further (XRD, EM, and ED results) and the specific surface areas (Fig. 3) decrease, due to the "filling" of the channels with sulfided species, as demonstrated elsewhere (*36*). Mo^{6+} may partially be responsible for oxidizing S^{2-} to elementary sulfur which can appear as an individual phase (Fig. 2d).

Not only does sulfidation proceed during the HDS reaction on less prereduced ($r = 0$, a-0.17, partly a-0.38, see Table 2) catalysts but further simultaneous reduction also occurs. This parallel reduction–sulfidation more effectively promotes surface sulfidation (Fig. 9) than bulk sulfur uptake (Fig. 4). The initially low specific surface areas of prereduced catalysts can only decrease but never increase in the following reaction (Fig. 3). Simultaneously, higher surface S/(Co + Mo) ratios are obtained in this process than in the sulfidation of highly prereduced catalysts (Fig. 9). For the latter process, a gas–solid reaction was proposed between the sulfur atoms arising from thiophene and the anion vacancies of the catalyst (46) which is in accordance with the suggestions of Lipsch and Schuit (*7*). If an anion vacancy of a reduced Mo species is filled with a sulfur atom, cobalt–oxythiomolybdates may be produced. Such species were, indeed, directly observed by XRD during the initial period of the run (Table 1). We propose that the initial maximum values of the conversion (Fig. 10, Table 1, and Ref. (*37*)) are due to the presence of these oxythiomolybdates. Their formation is easiest near $r = 0.5$; that is why the initial very pronounced synergy is manifested (Figs. 10 and 11). The electron micrograph of a catalyst $r = 0.50$ indicates the presence of incomplete MoS_2 layers on a $CoMoO_4$ matrix after 10 min H_2/T (Fig. 2c and Ref. (*36*)). Oxythiomolybdates may be the precursors of MoS_2. We propose that cobalt–oxythiomolybdates represent the most active HDS sites during the oxide–sulfide transition of unsupported catalysts. However, these compounds disappear relatively rapidly further on, parallel to the strongly decreasing HDS conversion.

The possible reasons of the activity loss are discussed in detail elsewhere (*37*). At the end of the run (Figs. 10 and 11), not only the activity decreases but also the synergy ceases to exist. In this stage the cobalt–oxythiomolybdate phase (Table 1) and/or any possibly present oxysulfides (*22, 29*) disappear. The parallel reduction–sulfidation discussed above seems to result in surface cobalt enrichment while sulfur incorporation into bulk does not. Surface cobalt enrichment may manifest itself in the appearance of separate Co_9S_8 phase (*36*); however, surface Co is not readily sulfided as seen from XPS spectra (Fig. 8) and the inversely proportional surface Co and S ratios (Fig. 9). The sulfidation of surface atoms may be hindered in this stage (low S ratios) but cannot influence the bulk sulfur content which is higher with higher Co content of the catalyst. It is assumed, therefore, that bulk sulfidation may be attributed to the formation of MoS_2 which promotes catalytic HDS and HYD (Fig. 12).

In general, the enrichment of surface cobalt in this, partially sulfided state may be responsible for the "plateau" of HDS activity at the end of the run (Figs. 10 and 12). Whatever the active sites may be in this state, clean Mo seems to be most active here. This stabilizing effect on the HDS conversion is almost independent of the composition in the mixed composition range. HYD selectivity, on the other hand, decreases linearly with increasing Co content; this can support the views (*31, 32*) that different kinds of active sites may be responsible for these processes.

ACKNOWLEDGMENTS

We thank Mr. L. Tóth for surface area measurements. Valuable discussions with Professor P. Tétényi, Drs. Z. Schay, I. Bertóti, R. Fréty, and J. Słoczynski are gratefully acknowledged.

REFERENCES

1. McKinley, J. B., *in* "Catalysis" (P. H. Emmett, Ed.), Vol. 5, p. 405. Reinhold, New York, 1957.
2. Gates, B. C., Katzer, J. R., and Schuit, G. C. A., *in* "Chemistry of Catalytic Processes," Chap. 5, McGraw–Hill, New York, 1979.
3. Grange, P., *Catal. Rev. Sci. Eng.* **21,** 135 (1980).
4. Delmon, B., *Amer. Chem. Soc., Div. Pet. Chem. Prepr.* **22,** 503 (1977), cited after Ref. (*3*).
5. Vissers, J. P. R., Bachelier, J., ten Doeschate, H. J. M., Duchet, J. C., de Beer, V. H. J., and Prins, R., *in* "Proceedings, 8th International Congress on Catalysis, Berlin, 1984," pp. II–347. Dechema, Frankfurt-am-Main, 1984.
6. Topsøe, H., and Clausen, B. S., *Appl. Catal.* **25,** 273 (1986).
7. Lipsch, J. M. J. G., and Schuit, G. C. A., *J. Catal.* **15,** 163, 179 (1969).
8. Korányi, T. I., Szilágyi, T., Manninger, I., and Paál, Z., *Polyhedron* **5,** 225 (1986).
9. Trifiro, F., Caputo, G., and Villa, P. L., *J. Less-Common Met.* **36,** 305 (1974).
10. Gajardo, P., Grange, P., and Delmon, B., *J. Chem. Soc. Faraday Trans. 1* **76,** 929 (1980).
11. Cimino, A., and de Angelis, B. A., *J. Catal.* **36,** 11 (1975).
12. Sotani, N., *Bull. Chem. Soc. Japan* **48,** 1820 (1975).
13. Sotani, N., and Hasegawa, M., *Chem. Lett.*, 1309 (1975).
14. Sotani, N., *Chem. Lett.*, 1039 (1977).
15. Brinen, J. S., and Armstrong, W. D., *J. Catal.* **54,** 57 (1978).
16. Chin, R. L., and Hercules, D. M., *J. Phys. Chem.* **86,** 3079 (1982).
17. de Beer, V. H. J., van der Aalst, M. J. M., Machiels, C. J., and Schuit, G. C. A., *J. Catal.* **43,** 78 (1976).
18. Gajardo, P., Mathieux, A., Grange, P., and Delmon, B., *Appl. Catal.* **3,** 347 (1982).
19. Arnoldy, P., de Jonge, J. C. M., and Moulijn, J. A., *J. Phys. Chem.* **89,** 4517 (1985).
20. Arnoldy, P., Franken, M. C., Scheffer, B., and Moulijn, J. A., *J. Catal.* **96,** 381 (1985).
21. Scheffer, B., de Jonge, J. C. M., Arnoldy, P., and Moulijn, J. A., *Bull. Soc. Chim. Belg.* **93,** 751 (1984).
22. Arnoldy, P., van den Heijkant, J. A. M., de Bok, G. D., and Moulijn, J. A., *J. Catal.* **92,** 35 (1985).
23. Arnoldy, P., de Booys, J. L., Scheffer, B., and Moulijn, J. A., *J. Catal.* **96,** 122 (1985).
24. Okamoto, Y., Shimokawa, T., Imanaka, T., and Teranishi, S., *J. Catal.* **57,** 153 (1979).
25. Jeziorowski, H., Knözinger, H., Taglauer, E., and Vogdt, C., *J. Catal.* **80,** 286 (1983).
26. Massoth, F. E., *J. Catal.* **36,** 164 (1975).
27. Hayden, T. F., and Dumesic, J. A., *J. Catal.* **103,** 366 (1987).
28. Delannay, F., *Appl. Catal.* **16,** 135 (1985).
29. Schrader, G. L., and Cheng, C. P., *J. Catal.* **80,** 369 (1983).
30. Miremadi, B. K., and Morrison, S. R., *J. Catal.* **103,** 334 (1987).
31. Massoth, F. E., and Murali Dhar, G., *in* "Proceedings, Climax 4th Intern. Conf. Chem. Uses Molybd." (H. F. Barry and P. C. H. Mitchell, Eds.), p. 343. Climax Molybdenum Co., Ann Arbor, MI, 1982.
32. Yang, S. H., and Satterfield, C. N., *J. Catal.* **81,** 168 (1983).
33. Wambeke, A., Jalowiecki, L., Kasztelan, S., Grimblot, J., and Bonnelle, J. P., *J. Catal.* **109,** 320 (1988).
34. Bussell, M. E., Gellman, A. J., and Somorjai, G. A., *J. Catal.* **110,** 423 (1988).
35. de Beer, V. H. J., Bevelander, C., van Sint Fiet, T. H. M., Werter, P. G. A. J., and Amberg, C. H., *J. Catal.* **43,** 68 (1976).
36. Günter, J. R., Marks, O., Korányi, T. I., and Paál, Z., *Appl. Catal.* **39,** 285 (1988).
37. Korányi, T. I., and Paál, Z., *in* "Proceedings, Cat. Petr. Ref. Conf. Kuwait, March, 1989." Elsevier, Amsterdam, in press.
38. Delannay, F., Damon, J. P., Masson, J., and Guille, J., *Appl. Catal.* **4,** 169 (1982).
39. Massoth, F. E., *in* "Advances in Catalysis" (D. D. Eley, P. W. Selwood, and P. B. Weisz, Eds.) Vol. 27, p. 265. Academic Press, New York, 1978.
40. Gajardo, P., Grange, P., and Delmon, B., *J. Catal.* **63,** 201 (1980).
41. Grimblot, J., Payen, E., and Bonnelle, J. P., *in* "Proceedings, Climax 4th Intern. Conf. Chem. Uses Molybd." (H. F. Barry and P. C. H. Mitchell, Eds.), p. 261. Climax Molybdenum Co., Ann Arbor, MI, 1982.
42. Scofield, J. H., *J. Electron. Spectrosc. Relat. Phenom.* **8,** 129 (1976).
43. Reilman, R. F., Msezane, A., and Manson, S. T., *J. Electron Spectrosc. Relat. Phenom.* **8,** 389 (1976).
44. Powell, C. J., *Surf. Sci.* **44,** 29 (1974).
45. Valyon, J., and Hall, W. K., *J. Catal.* **84,** 216 (1983).
46. Korányi, T. I., Manninger, I., and Paál, Z., *Solid State Ionics,* in press.
47. Frost, D. C., McDowell, C. A., and Woolsey, I. S., *Mol. Phys.* **27,** 1473 (1974).
48. Alstrup, I., Chorkendorff, I., Candia, R., Clausen, B. S., and Topsøe, H., *J. Catal.* **77,** 397 (1982).
49. Zingg, D. S., Makovsky, L. E., Tischer, R. E., Brown, F. R., and Hercules, D. M., *J. Phys. Chem.* **84,** 2898 (1980).